Influence of Wood Density on Backwater Rise due to Wood Accumulations upstream of a Retention Rack

Rebeca Mallqui[1], Erick Claros[2], Juan W. Cabrera[3]

Abstract

Wood accumulations in rivers can cause the blockage of natural or artificial hydraulic infrastructure. This phenomenon occurs recurrently in Amazonian rivers, which carry large quantities of wood during flood periods, which are retained in dams and river ports, causing the water level to rise and putting these structures at risk. As wood can correspond to different species, this article presents the results of a study on the effects of wood density on the rise in water level and the shape of the wood accumulation upstream of a laboratory-scale retention grid. The experiments were conducted under five different flow conditions in a variable-slope channel equipped with a retention grid, using artificial log sets with varying densities.

The reproducibility tests showed consistent results, with a mean relative standard error of 3.74% in the measurements of the relative backwater rise (i.e., change in water level with respect to the initial flow depth). The main findings indicate that backwater rise increases with the density of wood logs, while the compactness of the wood accumulation (represented by the ratio between the height and the length of the accumulation) also increases with log density. Finally, the equation proposed by Schalko et al. (2019) was adapted to include the effect of wood density.

This study highlights the importance of including wood log density in future flood risk studies.

[1]mmallqui@uni.pe, National University of Engineering, Lima, Peru
[2]erick.claros@uni.pe, National University of Engineering, Lima, Peru
[3]juancabrera@uni.edu.pe, National University of Engineering, Lima, Peru

Keywords

Backwater increase, large wood, driftwood, debris rack, scale experiments

1   Introduction

The transport of woody material in rivers is highly important in fluvial ecosystems (Gurnell et al., 2002). However, during extraordinary events this material can form accumulations capable of blocking natural and artificial structures, causing changes in the flow and geomorphology of the river. According to Lucía et al. (2015), the transport of logs in rivers originates from landslides on slopes, the erosion of banks and the entrainment of pieces during floods. When transportation occurs in semi-congested conditions, the logs move without interacting with each other. In contrast, when it occurs under congested conditions, large accumulations are observed in a single mass, which is more relevant for hazard analysis (Braudrick & Grant, 2000).

Logs transported in rivers with lengths greater than 1 m and diameters greater than 0.1 m are known as large wood (LW). Logs transported in the rivers of the Peruvian jungle with similar dimensions are known as "palizada" and their accumulation effects are evident in bridges, fluvial ports and dams of hydroelectric plants (see Figure 1). To address this issue, it is recommended to first thoroughly study the obstruction mechanisms associated with LW transport (Gschnitzer et al., 2017).
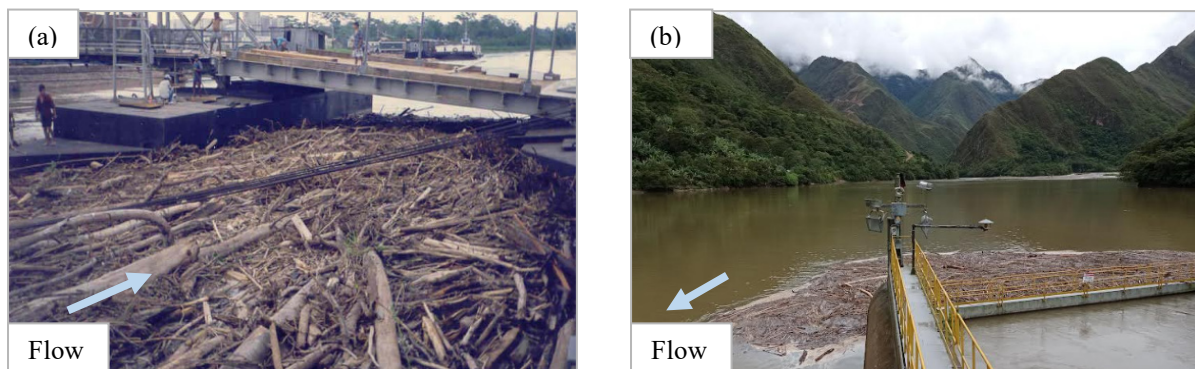

Figure 1: Wood accumulation: (a) fluvial port in Huallaga River, Peru (Consortium Hidrovia Huallaga, 2005) (b) Tulumayo dam, Chimay hydroelectric power plant, Junin, Peru (photo courtesy by Author)

One of the effects of wood accumulation upstream of a retention structure is backwater rise, which appears as a gradually varied flow profile under certain conditions of flow rate, channel slope and flow regime (Chow, 1959). Backwater rise and the flow velocity beneath the jam are key factors in determining the ecological, geomorphic and flood-related impacts of wood accumulation (Follett et al., 2021). In the present study, backwater rise is caused by an obstruction in a gently sloping channel under both subcritical and supercritical flow conditions. Parameters that influence backwater rise due to wood accumulations in flume experiments are associated with flow and log properties (Al-Zawaidah et al., 2021; Hartlieb, 2017b; Schalko et al., 2019; Schmocker & Hager, 2013), with the Froude number being the most influential. Higher Froude numbers result in greater backwater rise.

To begin with, Schmocker & Hager (2013) identified two phases in the formation of wood accumulation upstream of a retention rack: the first, during which the main backwater rise occurs, and the second, when a long wood carpet forms but has no significant influence on backwater rise.

Subsequently, Hartlieb (2015) developed a risk analysis on the transport of wood in rivers, including a study of consequences of blockages in the structures. Based on this, experiments on the effects of wood density on the headwater level upstream of a spillway were carried out. The results showed increased headwater levels and reduced discharge flow through the structure due to the increase in wood density. Hartlieb (2017) specifically studied the influence of accumulation shape on backwater rise and proposed a relation between the dimensions of debris accumulation, the relative debris density and the initial Froude number. According to the results, the higher the initial Froude number the larger the debris density, the more compact the debris jam, and the higher its backwater effect.

As a key point, Schalko et al. (2018) systematically evaluated a series of parameters and proposed a design equation to estimate the backwater rise upstream of a retention rack due to predefined box-shaped accumulations, which depends on the Froude number, large wood accumulation length, log diameter, fine material, loose wood volume and solid wood volume. Later, Schalko et al. (2019) proposed a variation of the design equation to estimate backwater rise due to natural

wood accumulations, including an accumulation type factor, initial flow depth and channel width. In the same study, the characteristic volume (V_c) was analyzed, which refers to the amount of wood that produces the maximum increase in backwater rise.

For their part, Al-Zawaidah et al. (2021) investigated the geomorphic changes caused by the accumulation of different densities of wood and plastics at a vertical rack. The results showed that the maximum scour depth was observed in the presence of light accumulations (density $< 1000\,kg/m^3$) and the minimum scour depth was observed with dense accumulations (density $> 1000\,kg/m^3$). The study highlighted the importance of considering the accumulation density as a critical factor in the prediction of geomorphic changes within the riverine system.

The influence of the Froude number on wood accumulation dimensions was also studied by Panici & de Almeida (2018), who carried out flume experiments on wood accumulation upstream of a bridge pier and showed that for low values of the Froude number, accumulation length and width are the highest. Moreover, the experiment performed with the highest value of relative wood density resulted in an accumulation that was up to 30 % deeper than those formed with the lowest values of relative wood density.

In summary, recent research has addressed the influence of the density of floating materials on the increase in backwater for different steady flow conditions, including natural wood, plastic waste and artificial wood. However, it was deemed necessary to extend the study to accumulations with a wider range of wood densities. Therefore, the aim of this research was to evaluate the influence of wood density on backwater rise and the characteristics of the accumulation upstream of a retention rack. For this purpose, flume experiments were conducted with artificial logs covering a wide range of wood density values.

The remainder of this work is structured as follows. Section 2 presents the dimensional analysis with the parameters evaluated in this study, Section 3 explains the research methodology. Next, Section 4 shows the main findings. The summary and interpretation of the results are discussed in Section 5. The main conclusions are outlined in Section 6.

2   Background and Theory

According to the analysis developed by Schalko et al. (2018), backwater rise is a function of the bulk factor ($a = \frac{V_l}{V_s}$), the initial Froude number (F_o), relative volume of fine organic material (FM), and the flow diversion parameter $\left(\mu = \frac{V_S}{h_o B d_L}\right)$. This relationship can be expressed as:

$$\frac{\Delta h}{h_0} = f\left(a, F_o, FM, \frac{V_S}{h_o B d_L}\right) \tag{1}$$

Where $\Delta h/h_0$ is the relative backwater rise, Δh is the increase of flow depth, h_0 is the approach flow depth, $F_o = v/\sqrt{g\,h_0}$ is the initial Froude number, g is the acceleration of gravity, v is the velocity of the flow, V_s is the solid volume of the log accumulation, V_l is the loose volume, h_o the initial flow depth, B the width channel and d_L the log diameter.

In the present investigation, the influence of relative wood density will be evaluated and incorporated according to the following modified relationship:

$$\frac{\Delta h}{h_0} = f\left(a, F_o, FM, \frac{V_S}{h_o B d_L}, \frac{\rho_L}{\rho_W}\right) \tag{2}$$

Where ρ_L/ρ_W is the relative wood density, ρ_L is the log density and ρ_W is the water density. This last equation can be expressed in a functional way:

$$\frac{\Delta h}{h_o} = \left(\frac{\rho_L}{\rho_W}\right)^{k_1} a^{k_2} F_o^{k_3} \left(\frac{V_s}{h_o B d_L}\right)^{k_4} FM^{k_5} \tag{3}$$

Where k_i are exponents that will be explained in the results section.

3   Methodology

A program of 60 tests was carried out in 20 different scenarios, varying the density of the wood, the Froude number and the initial flow depth. For this purpose, a model was set up using a variable slope channel, a retention rack and artificial logs manufactured with 3D printers at the Didactic Area of the National Hydraulics Laboratory of the National University of Engineering (Lima, Peru).

3.1 Model Configuration

The model consists of a 10.6 m long, 0.5 m high and 0.25 m wide channel with a bottom slope that can be varied manually. A flow stabilizer box is located at the inlet of the channel to reduce turbulence. The inflow discharge was controlled with a valve capable of handling up to 0.040 m³/s. Downstream conditions were controlled with a louvered gate. The log retention rack was located 6.3 m downstream of the channel inlet and was composed of eight vertical stainless-steel bars, which were equally spaced and had a diameter of 3 mm. The artificial logs were incorporated into the flow 4.7 m upstream of the retention rack. A basket was installed at the outlet of the channel to collect the artificial logs that passed through the rack to obtain the percentage of retained logs. Figure 2 shows the test scheme proposed for the experiment.
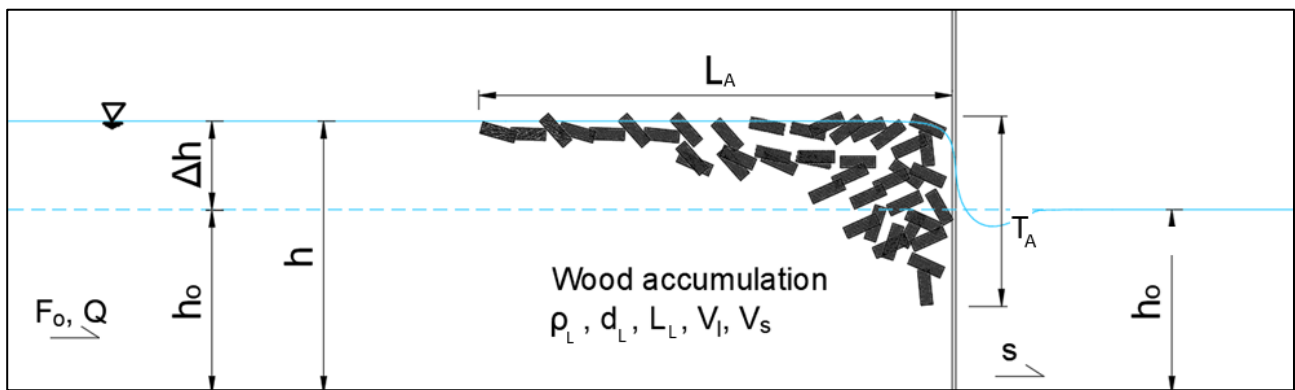

Figure 2: Experimental setup and notations

The variables associated with the initial conditions are the initial flow depth (h_o), initial Froude number (F_o) and flow rate (Q). The characteristics of the wood accumulation are log density (ρ_L), log length (L_L), log diameter (d_L), solid volume (V_s), loose volume (V_l), accumulation length (L_A), accumulation thickness (T_A) and the channel slope (s). F_A was considered for the Froude number after formation of the LW accumulation upstream of the rack.

The flow depth was measured with a needle gauge featuring a measurement accuracy of ± 0.1 mm and the flow rates were measured with a triangular weir having a measurement accuracy of ± 0.1 % for a maximum flow rate of 0.017 m³/s.

The model studied in the present investigation is not related to a particular prototype or case study; even so, the length of the artificial logs was carefully selected to allow the formation of a jam that resembles real ones. However, if a scale of 1:30 is considered, the length of the prototype log would be 1.8 m and the diameter 0.3 m.

To ensure the retention of logs in the rack, the log length was selected to be at least 1.5 times greater than the open spacing between the rack bars (Lange & Bezzola, 2006). The percentage of retained logs varied in each scenario, according to the results shown in Figure 3.
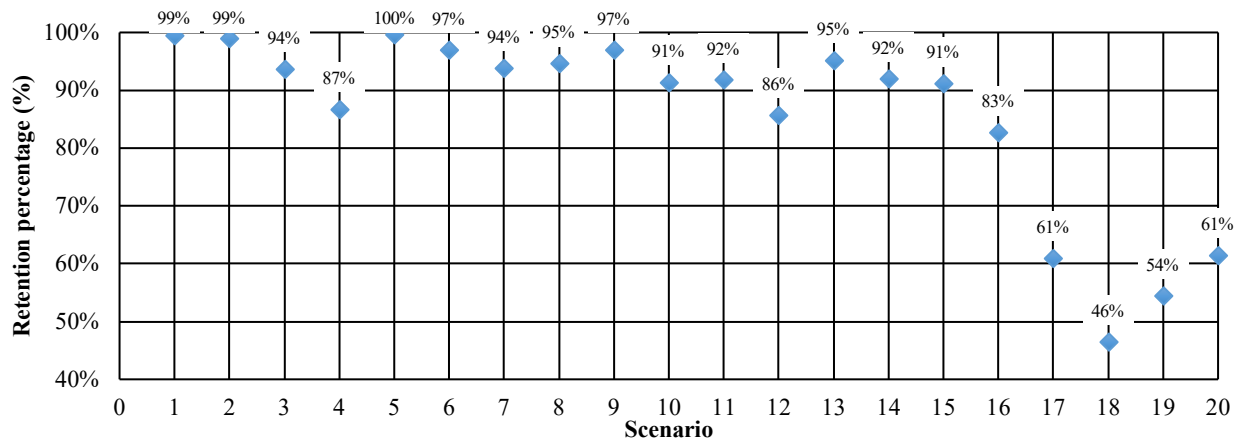
Figure 3: Percentage of log retention per scenario

According to the results, almost all the added logs were retained when the initial flow regime was subcritical, and about half were retained when the regime was supercritical.

It is important to highlight that the estimated loose volumes (V_l) and solid volumes (V_s) for each scenario correspond to the logs retained upstream of the retention grid, i.e., the solid volume represents the space occupied by the retained logs, and the loose volume is the final volume that forms the accumulation of retained logs, including the space within the internal voids. It is also important to emphasize that fixed volumes were used during the test program, that is, at the beginning of all experiments, the same total solid volume was added upstream of the retention grid.

An additional consideration is that the logs were incorporated into the center of the channel and parallel to the walls to avoid side effects. Considering these factors, a log length (L_L) of 0.06 m was selected, which represents 25 % of the flume width. Moreover, this ratio lies within the range of values used in similar studies. For instance, Schalko et al. (2021) used logs of various lengths whose ratios to their flume width ranged between 12.5 % and 50 %, while Schmocker & Hager (2013) performed their experiments with ratios between 13 % and 33 %.

As mentioned, no scaling factor was defined, and the experiments were designed to explore conditions occurring in a typical river that transports LW. In free surface flows, the effects of gravity are predominant and similarity between the model and prototype is usually developed with Froude similarity. Scaled models based on Froude similarity may overestimate the effects of surface tension and fluid viscosity, since the use of another fluid with such scaled properties is not possible. For discharge effects, surface tension is negligible provided that the flow height exceeds 0.02 m (Furlan, 2019). In that regard, the model considers flow heights within the proposed limits to avoid the effects of surface tension and viscosity on flow discharge.

3.2 Test Program

To establish the 20 test scenarios, four different log densities and five different Froude numbers were predefined, split over two initial depths. The Froude numbers were experimentally obtained by adjusting the flow rate, channel slope and downstream weir. Each scenario was repeated three times to evaluate the reproducibility of the tests, making a total of 60 simulations. The log dimensions were 0.06 m in length and 0.01 m in diameter and the total solid volume accumulation was 0.0033 m³. These parameters were kept constants for all scenarios. The initial parameter values for the 20 scenarios are shown in Table 1.

Due to the randomness of this type of study, the experimental measurements of each parameter are associated with uncertainty. Relative standard error $e * (\%)$ was calculated according to the following expression:

$$e * (\%) = \frac{\sigma_n}{\bar{x} * \sqrt{n}} * 100 \qquad (4)$$

For each group of scenarios with the same Froude number, values below 1 % were obtained. The results are shown in Table 1.

Table 1: Scenarios and test configurations. Values in brackets indicate relative standard error (%)

Scenario	Log density ρ_L (kg/m3)	Discharge Q (m3/s)	Slope s (%)	Approach flow depth h_o (m)	Approach Froude number F_o
1 - 4	400; 600; 800; 950 resp.	0.005 (0.19)	0.02	0.10 (0.09)	0.2 (0.25)
5 - 8	400; 600; 800; 950 resp.	0.004 (0.26)	0.0	0.06 (0.31)	0.3 (0.62)
9 - 12	400; 600; 800; 950 resp.	0.01 (0.38)	0.02	0.10 (0.19)	0.4 (0.42)
13 - 16	400; 600; 800; 950 resp.	0.006 (0.14)	0.15	0.06 (0.49)	0.5 (0.70)
17 - 20	400; 600; 800; 950 resp.	0.017 (0.26)	0.8	0.06 (0.40)	1.3 (0.72)

3.3 Manufacture of artificial logs

Artificial logs manufactured with 3D printers were used to simulate the accumulation of woody material. These pieces were manufactured with four different densities, all less than 1000 kg/m^3, to ensure buoyancy and transport. Each density was represented by a color: green (400 kg/m^3), blue (600 kg/m^3), yellow (800 kg/m^3) and red (950 kg/m^3). The density values considered span a range that includes species densities in European (Ruiz-Villanueva et al., 2016) and Amazonian (Moya Roque et al., 2008) watersheds. Each group consisted of 700 artificial logs of the same dimensions, resulting in a total solid volume of 0.0033 m^3. In this case, the accuracy of the density parameter comes from manufacturing and the highest variability is found in the group with the lowest density (7.5 %). The values of manufacturing accuracy for log densities are shown in Table 2.

Another important point is the variability in the weight due to the moisture absorption of the logs. This was evaluated using 3 samples from each density group in a dry state and after one hour submerged, because the maximum test time per density group was one hour per day. The obtained absorption percentages can be observed in Table 2.

Table 2: Manufacturing accuracy of log density and absorption percentage

Log density ρ_L (kg/m^3)	Manufacturing accuracy (%)	Absorption percentage (%)
400	7.5	1.8
600	5.0	0.2
800	3.8	0.2
950	3.2	0.8

As can be seen, the maximum absorption percentage (%) is a quarter of the maximum manufacturing accuracy. All the logs were 3D-printed with PLA (Polylactic acid) with variations in the wall thickness and fill density to obtain different densities.

3.4 Test Procedure

The experimental procedure can be summarized in the following steps:

- Regulation of flow rate (Q), channel slope (s), initial approach flow depth (h_o) and pre-established Froude number (F_O).

- Manual addition of packets of artificial logs of 8 % - 10 % of the total solid volume (between 60 and 70 pieces) every 15 seconds, 4.7 m upstream of the retention rack. The number of artificial logs collected in the outlet basket is counted to determine the retention percentage and they were not reincorporated into the flow.

- Measurement of the flow depths 0.30 m upstream of the retention rack by means of the limnimeter.

- Measurement of the accumulation dimensions (length, thickness and lateral area) through photo analysis and estimation of the accumulation characteristics (solid volume and loose volume). Solid volume (V_s) was calculated

using the equation of the cylinder multiplied by the number of retained logs (Livers et al., 2020). Loose volume (V_l) was estimated as the product of the lateral area of accumulation and channel width. The lateral area was estimated by photo analysis.

4   Results

The effects of wood density on accumulation thickness, length, characteristic volume, and compactness are analyzed in this section.

4.1 Reproducibility Tests

Reproducibility tests found that the relative standard errors ($e*$) of the relative backwater rise for all tests ranged from 0.23 % to 11.01 %, with a mean value of 3.74 %. These values are below the range recommended by Schalko et al. (2018), who consider standard error percentages below 15 % acceptable for tests with wood accumulations. Figure 4 shows that the highest relative standard errors are found in the scenarios with supercritical flow.
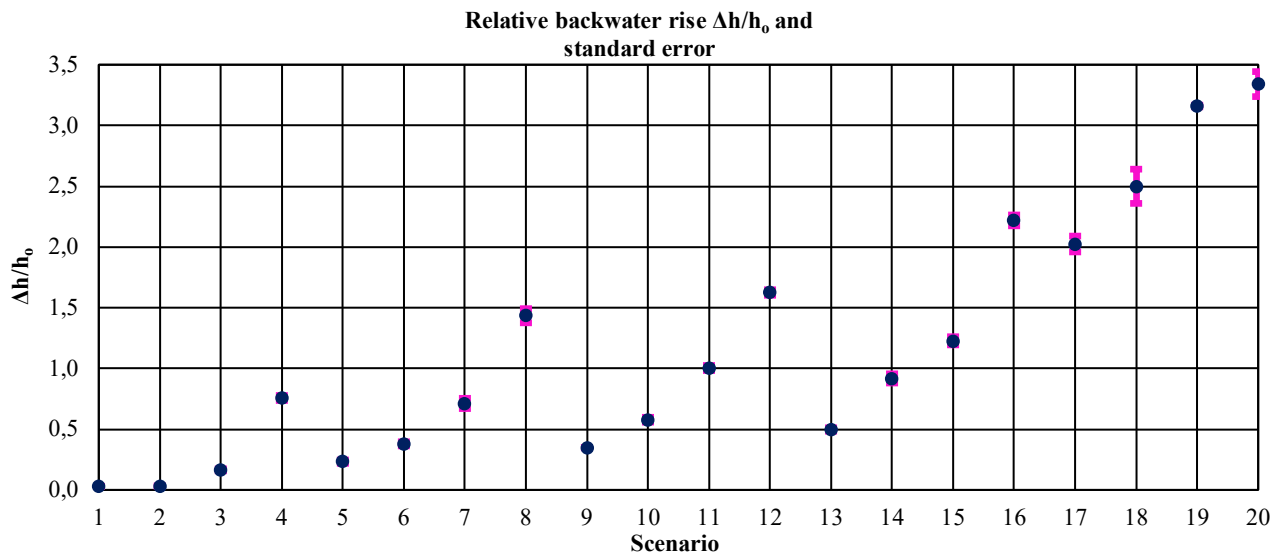

Figure 4: Reproducibility error of the backwater rise for each test scenario

4.2 Effects of wood density on the accumulation characteristics

4.2.1   Thickness and length accumulation

The first notable observation during the experiments was the variation in the shape of the accumulations with the wood density. This may be due to the influence of wood density on the buoyancy of the artificial logs, which also influences the arrangement of the wood pieces in the stream, as shown in Figure 5. At first glance, the accumulation of artificial logs with a higher density has a shorter length (L_A) and greater thickness (T_A).
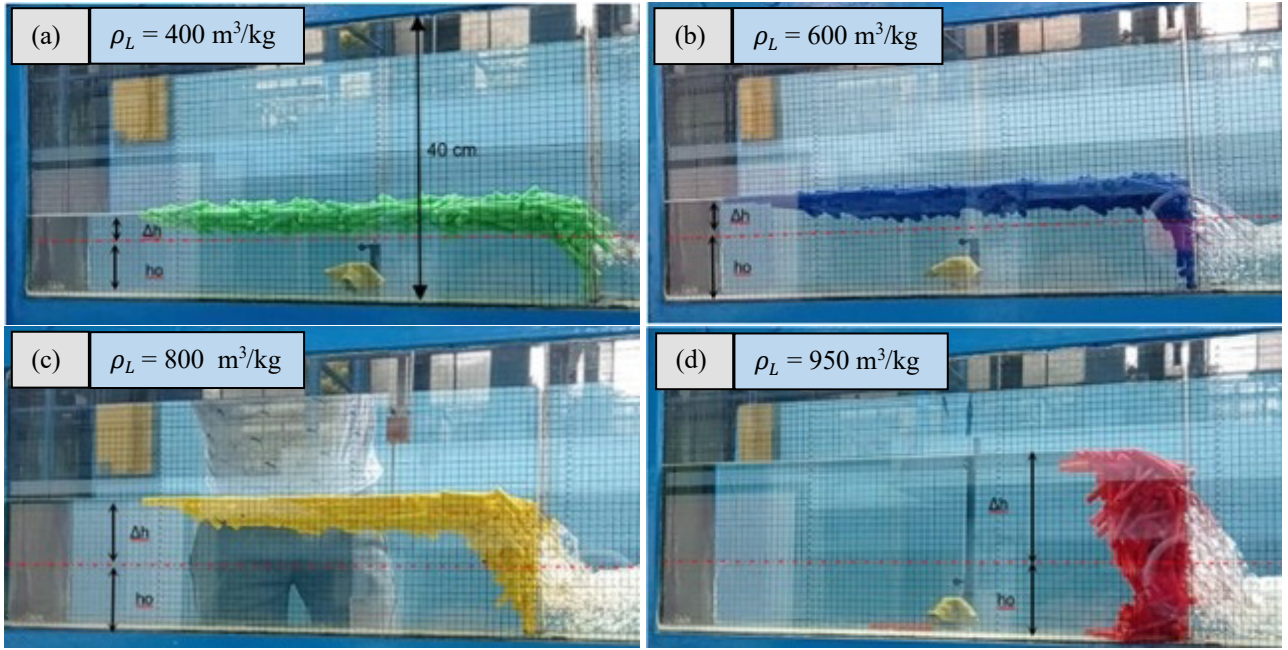
Figure 5: Formation of wood accumulations for: a) scenario 9 (ρ_L = 400 kg/m³, F_o= 0.4), b) scenario 10 (ρ_L = 600 kg/m³, F_o= 0.4), c) scenario 11 (ρ_L = 800 kg/m³, F_o= 0.4) and d) scenario 12 (ρ_L = 950 kg/m³, F_o= 0.4)

According to the results, the accumulation thickness (T_A) increases with increasing wood density (ρ_L) and initial Froude number (F_o); this can be seen in Figure 6a. Furthermore, the accumulation thickness is higher for h_0 = 0.10 m compared to the accumulation thickness obtained with h_0 = 0.06 m. However, values are compensated when divided by the initial height (Figure 6b).
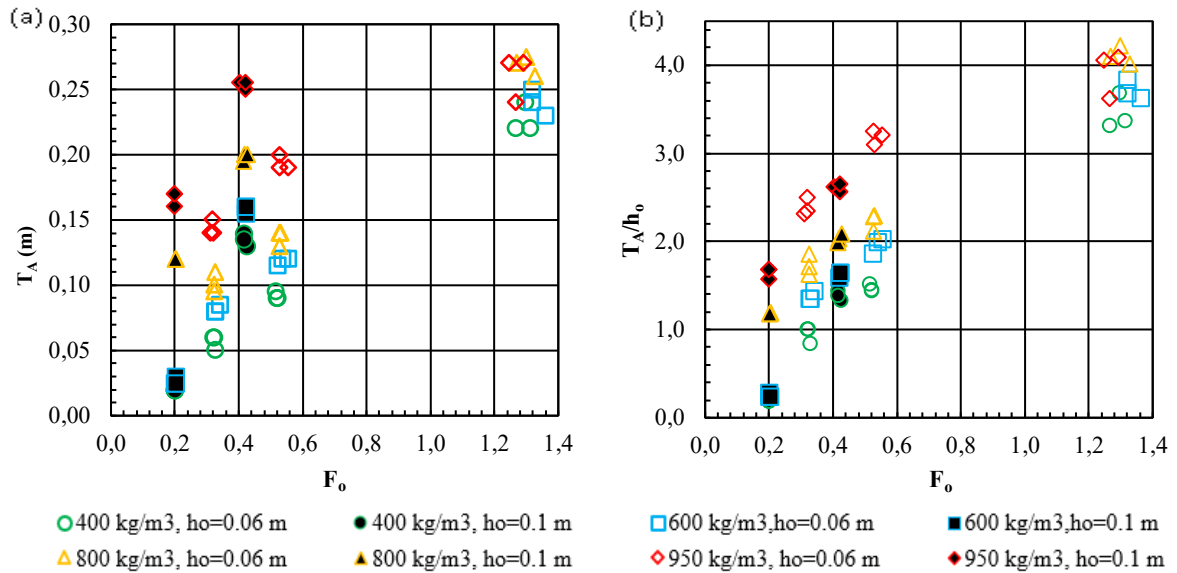

Figure 6: a) Froude number vs. accumulation thickness (T_A), b) Froude number vs. dimensionless T_A, for different log densities

Another finding is that the accumulation thickness (T_A) covered almost the whole flow depth (h) for all experiments except for scenarios 1 and 2, where the accumulation thickness was the minimum (see Figure 7) because the Froude number is 0.2 and log densities are the lowest (400 kg/m³ and 600 kg/m³).
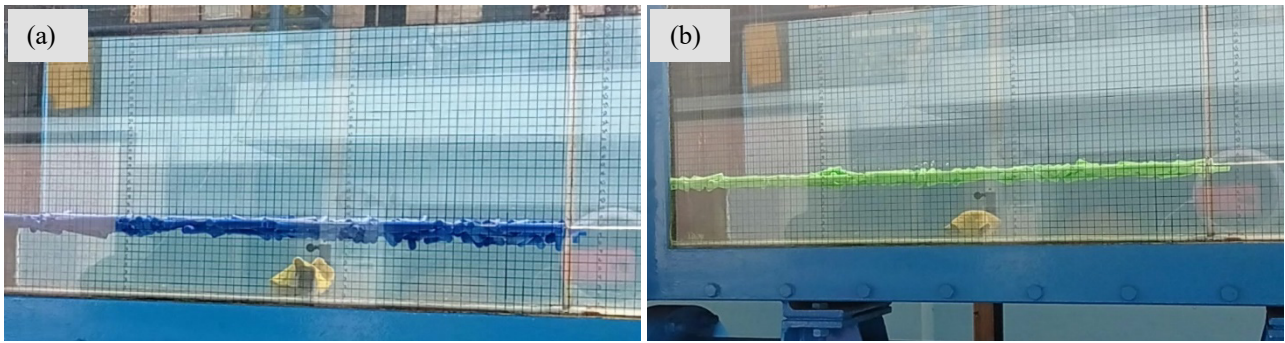
Figure 7: Accumulation for: a) scenario 1 (ρ_L= 400 kg/m³, F_o= 0.2), b) scenario 2 (ρ_L= 600 kg/m³, F_o= 0.2)

Similarly, in most experiments, T_A exceeded the initial flow depth (h_0) by up to a factor of four. This considerable difference shows that the log accumulation can have a high impact on defining the characteristics of the flow through an obstruction. In that sense, the relative backwater rise and the dimensionless accumulation thickness (T_A/h_0) adjust to a relatively linear relationship (R^2 = 0.94), which is evidenced in Figure 8.
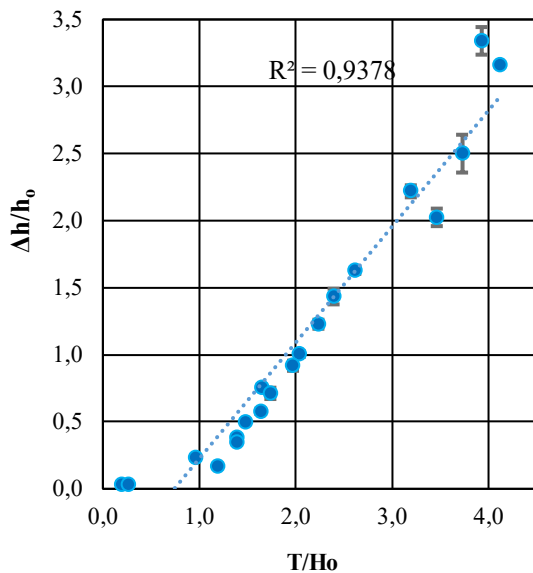

Figure 8: Accumulation thickness (T_A) vs. relative backwater rise $\Delta h/h_o$.

Regarding accumulation length (L_A), this decreases at larger initial depths (for a fixed wood volume), except for scenario 1, because logs tend to occupy the entire water column. Thus, at larger initial depths, the accumulation has more vertical space, leading to a smaller accumulation length. The results can be seen in Figure 9a. Then, similarly to the accumulation thickness (T_A), the length was non-dimensionalized using the initial water depth (h_0) and compared with the Froude number; however, in contrast, L_A/h_0 exacerbates the decrease in the accumulation length with respect to the initial water depth (see Figure 9b).
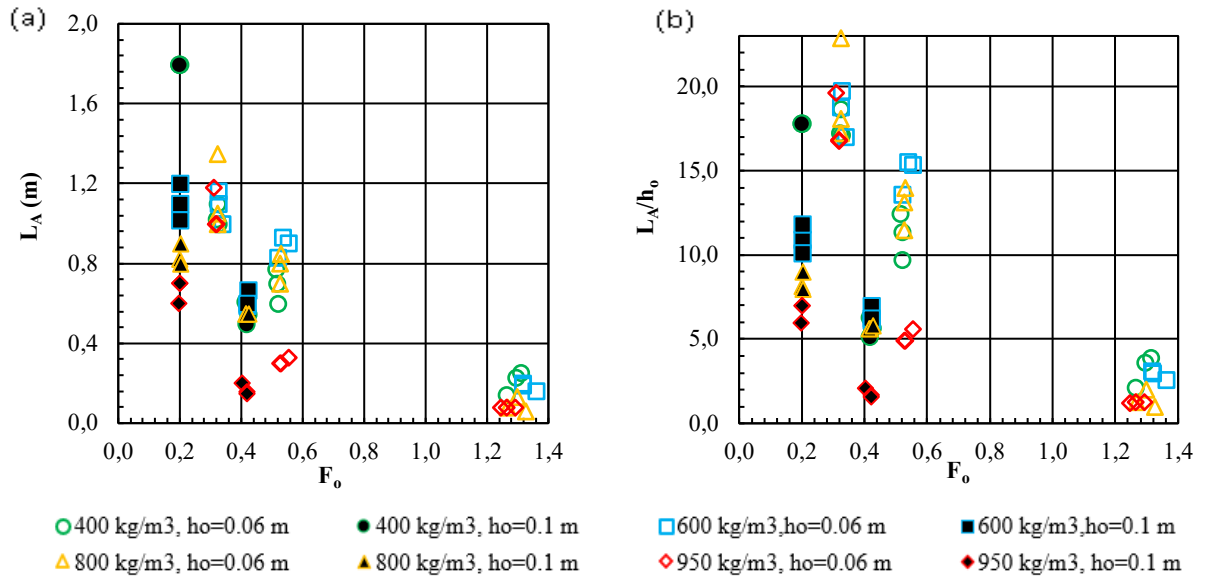
Figure 9: (a) Froude number vs. accumulation length L_A (m), (b) Froude number vs. dimensionless L_A, for different log densities.

Figure 10 shows that the relative backwater rise decreases with dimensionless length. The trend line follows a potential relation with $R^2 = 0.65$.
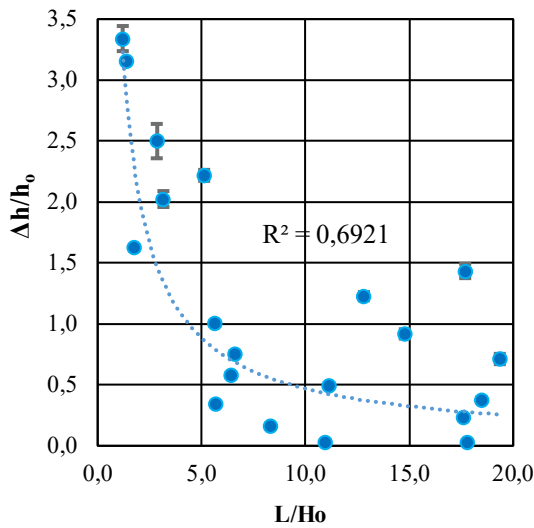

Figure 10: Length accumulation L_A vs. relative backwater rise $\Delta h / h_o$

To sum up, tests performed with fixed volumes for two initial water depths generate two populations of dimensionless volumes, which can be seen in Figure 6a and Figure 9a. In addition, accumulation length and thickness were compared with backwater rise as a reference to observe how backwater varies with respect to both accumulation dimensions in Figure 8 and Figure 10.

4.2.2 Characteristic volume

The carpet length increases, especially after the solid volume (V_s) exceeds the characteristic volume (V_c). In the present study, V_c was estimated using the formula by Schalko et al. (2019) for channels with fixed bed and $F_o = 0.3 - 1.5$ ($R^2 = 0.89$):

$$V_c = 3.1 * F_o * (B * h_o^2)$$ (5)

Figure 11 shows that the Froude number with large wood accumulation present (F_A) decreases with increasing wood density. For each density, F_A decreases for $1 \geq V_s/V_c$ and then remains constant.
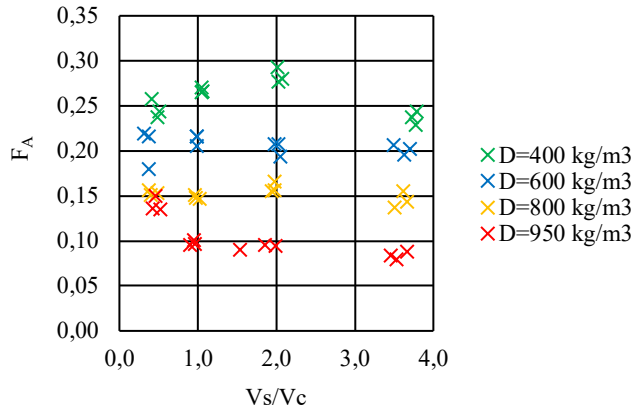

Figure 11: a) V_s/V_c versus F_A for different densities and b) V_s/V_c versus L_A/h_o.

It can be observed that the flow regimes are subcritical during wood accumulation for all simulations, regardless of the initial Froude number. In addition, it should be noted in Figure 11 that the upstream Froude numbers of all tests are independent of the hydraulic conditions and dependent on wood density. In other words, irrespective of the initial hydraulic conditions, if enough logs are added, backwater rise continues until a constant upstream Froude number is reached. This can be compared with the formation of a wood accumulation: when the characteristic volume is reached, the remaining logs form a longer carpet.

4.2.3   Compactness

Compaction was analyzed as the relationship between the thickness and the length of the accumulation (T_A/L_A) (Hartlieb, 2017). According to the reproducibility results, the relative standard error percentages for compactness are between 0 % and 10.7 % for the scenarios with subcritical flow (scenario 1 - 16) and values between 3.9 % and 19.5 % for the scenarios with supercritical flow (scenario 17 - 20). In addition, a trend of increasing compactness with wood density was observed for each Froude number and initial flow depth, as shown in Figure 12.

As described in section 4.2.1, L_A decreases with initial height (h_0) and T_A increases with h_0. Consequently, the compactness (T_A/L_A) is higher at greater initial depths (see Figure 12, the compactness at $h_0 = 0.1$ m vs. that at $h_0 = 0.06$ m). Furthermore, compactness strongly increases with the Froude number. While it is not possible to establish a direct relationship between T_A/L_A and h_0 considering the data of the present investigation, compactness is influenced by wood density and the Froude number.
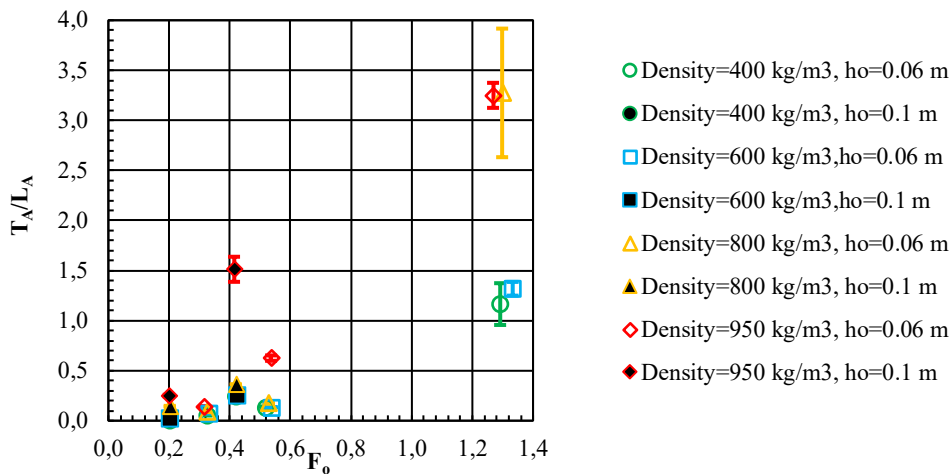

Figure 12: Froud number vs. compactness with standard error bars

To analyze the effects of wood density on accumulation compactness, the relationship proposed in the dimensional analysis of Hartlieb (2017) was used. Considering the data measured in the present investigation, a non-linear regression analysis was carried out using an R package, which utilizes the Gauss-Newton algorithm, to determine the coefficient $C_{T/L}$ and exponents m and n in Equation (6):

$$\frac{T_A}{L_A} = C_{T/L} F_o{}^m \left(\frac{\rho_L}{\rho_W}\right)^n \tag{6}$$

Obtaining equation (7):

$$\frac{T_A}{L_A} = 2.5 \, F_o^{1.7} \left(\frac{\rho_L}{\rho_W}\right)^{1.7} \tag{7}$$

Where $C_{T/L}$ is the proportionality constant and ρ_W is the water density (1000 kg/m³). The obtained values of m and n indicate a great influence of the initial Froude number and the relative wood density on the accumulation compactness. Moreover, Figure 13 shows the relationship between the experimental compactness values and the values predicted from Equation (7) with a precision range of 30 % and $R^2 = 0.90$.
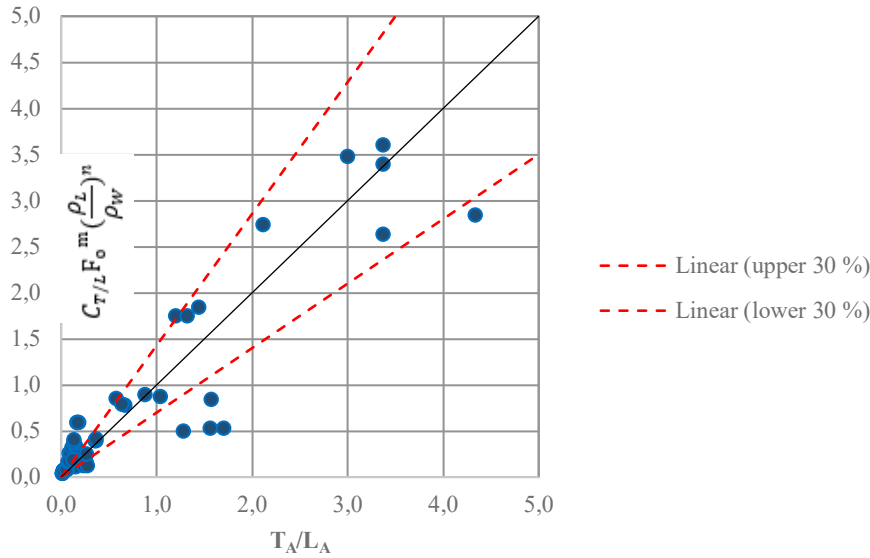

Figure 13: Experimental compactness values vs. values predicted with Equation (7)

4.3 Effects of wood density on backwater rise

To predict the relative backwater rise, the equation proposed by Schalko et al. (2019) was adapted to include the effect of wood density.

Considering the dimensional analysis of Section 2, the systematic experiments of Schalko (2019) yielded the values of $k_2 = -1, k_3 = 1, \; k_4 = \frac{1}{3}, k_5 = 1$ for Equation (3), for $F_o = 0.2 - 1.4$ with $R^2 = 0.97$.

$$\frac{\Delta h}{h_o} = C_1 \left(\frac{\rho_L}{\rho_W}\right)^{k_1} 5.4 \frac{F_o \left(\frac{V_S}{h_o B d_L}\right)^{\frac{1}{3}} (9FM + 1)}{a} \tag{8}$$

Additionally, such analysis included an accumulation type factor (f) that can depend on the density of logs. In that regard, in the present investigation, a relationship between accumulation type factor and relative density was found, making $C_1 = 0.64$ and $k_1 = 1$ in Equation (8), obtaining the new Equation (9) with $R^2 = 0.96$:

$$\frac{\Delta h}{h_o} = 3.48 \left(\frac{\rho_L}{\rho_W}\right) \frac{F_O \left(\frac{V_s}{h_o B d_L}\right)^{\frac{1}{3}} (9FM + 1)}{a} \tag{9}$$

It should be noted that the adapted equation is applicable only for fixed bed channels, that is, where erosion does not occur. The experimental backwater rise values, and the values predicted from the modified equation were compared and are shown in Figure 14b for a 30 % prediction range.
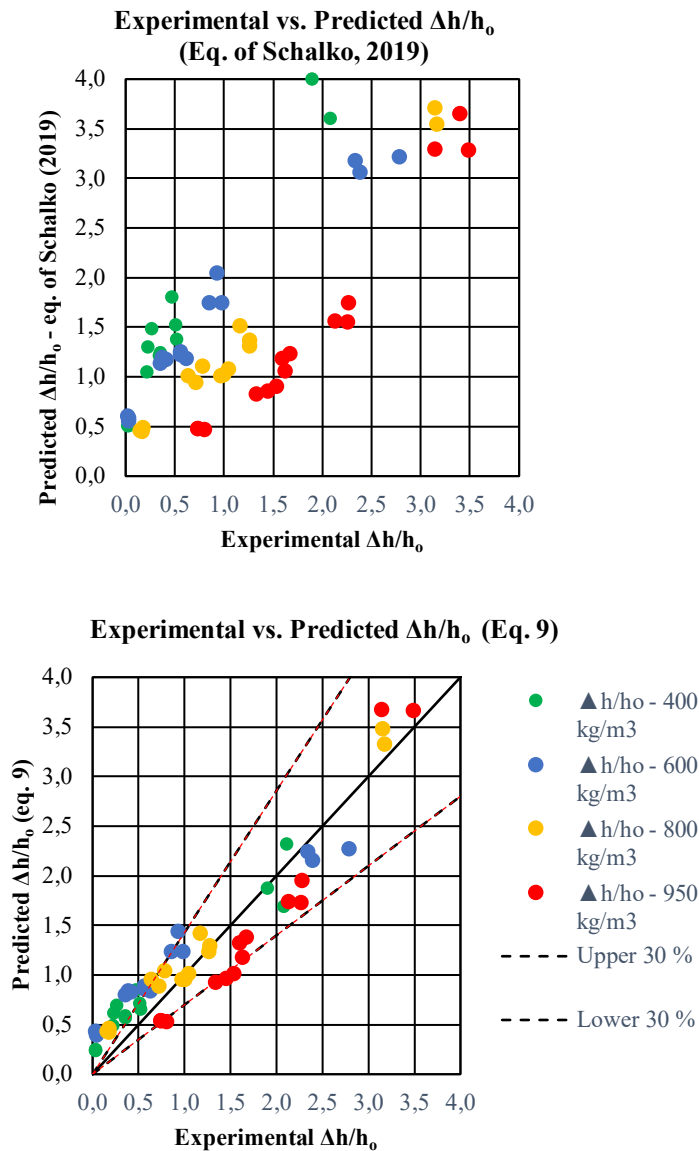

Figure 14: a) Relative backwater rise predicted by the equation of Schalko (2019) vs. experimental values, b) Relative backwater rise values Schalko (2019) predicted by modified equation (9) vs. experimental values.

The linear trend was found to offer a better correlation between relative density and the accumulation type factor. A potential relationship would only increase the dispersion of the data. Figure 14a shows that results predicted by the original equation in Schalko (2019), where significant dispersion is observed, while in Figure 14b the data collapse to the same line when relative wood density is included in Equation (9).

5   Discussion

5.1   Interpretation of Experimental Design and Materials

The percentage of retained logs was influenced mainly by the initial Froude number. It was observed that almost all the added logs were retained when the initial flow regime was subcritical and about half were retained when the regime was supercritical. This affects the volume of wood accumulation and the area of blockage in the channel. Regarding the backwater results, if the percentage of retained logs were higher for supercritical flow, the increase in backwater rise would be greater.

The range of log densities defined in this study, from 400 kg/m³ to 950 kg/m³, aimed to encompass the density values of different floating species considered in previous studies. Thanks to this, it was possible to identify the most unfavorable scenario for overflow risk, despite the limitations in floating material volume and channel height.

Concerning 3D printing, it allowed the manufacturing of elements with different densities for each scenario considered. PLA is a cheap material and biodegradable in the long term. To avoid the absorption of the pieces, it is recommended to adjust the wall thickness further or use another waterproof printing material, such as PVB (polyvinyl butyral).

Regarding the water absorption capacity of PLA, a maximum weight increase of 1.8 % due to water absorption was found, which is less than the average relative standard error of 3.4 % in backwater rise for scenarios where the log density is 400 kg/m³. This limited absorption is an important advantage for controlled experiments compared to natural wood, which absorbs more water over time, affecting the results.

5.2   Key Findings and Comparison with Literature

According to the results obtained, the highest percentages of error are presented in scenario 2 (11.01%), scenario 5 (6%), scenario 7 (5.94%) and scenario 18 (5.64%). These percentages do not seem to be influenced by flow conditions or wood density. One explanation is that the errors are related to manual measurements and to the uncertainty inherent in experiments with floating material accumulations (random movement of logs in the channel).

Follett et al. (2021) studied the flow distribution and water level rise upstream of an accumulation. The results showed that the backwater rise increases with jam resistance, which forces a greater discharge beneath the jam. In the present study, the height of the gap decreases with the accumulation thickness, which causes the flow resistance to be greater.

Panici & de Almeida (2018) obtained a 30 % variation in the wood accumulation thickness in their experiments due to the variation in wood density, whereas in the present investigation a variation of up to 88 % was obtained.

It is novel that the results show that the upstream Froude number (corresponding to the flow with wood accumulation present) of all tests is independent of hydraulic conditions but dependent on wood density. This finding can be useful for backwater rise predictions in future research.

Some findings provided insights into the influence of different initial depths on backwater rise. For a given F_O and dimensionless wood volume, the approach flow depth h_o has no effect on $\Delta h/h_o$ (Schalko et al., 2018). This was verified with the data measured in the present investigation.

Regarding the influence of wood density on the dimensions of the accumulation, a clear difference in the shape of the accumulation was observed for different densities in the experiments. It can be seen that accumulations become shorter and thicker for increasing wood density. Concerning the influence of the compactness, a relationship between the density of the wood and the compactness of the accumulation was found. This was achieved by non-linear regression, obtaining exponents greater than 1, which demonstrates the strong dependence of the initial Froude number and the density of the wood on the compactness.

6   Conclusions

The relative standard error percentages in the relative backwater rise values obtained from the reproducibility tests are limited and within the range recommended (15 % for tests with natural accumulations of wood). This was achieved by using 3D- printed logs that have uniform properties and lower absorption.

The tests performed with fixed volumes for two initial water heights generated two populations of dimensionless volumes. In addition, accumulation length and thickness were compared with backwater rise as a reference to observe how backwater varies with respect to accumulation thickness and length. According to the results, the decrease in the accumulation length is exacerbated when the relative length (L_A/h_0) is divided by the initial height, and the trend of the relative thickness (T_A/h_0) is compensated when divided by the initial height.

The results show that the compactness of the accumulation increases with the density of the wood. To obtain a specific relationship, the parameters of the dimensional equation presented by Hartlieb (2017) were determined using data measured in the present investigation.

It has been shown that the inclusion of the relative wood density in the original equation of Schalko et al. (2019) collapses the results of the different densities on the same line, which also demonstrates the dependence of the density of the wood on the relative backwater rise.

7   Recommendation

The use of 3D printers is recommended as an option for manufacturing small artificial pieces that would otherwise be very complex to build.

It is recommended to evaluate scour beneath wood accumulation, considering the maximum value of local species density, as this is when the gap under the accumulation is reduced.

The study of parameters that influence the increase in backwater rise, including wood density, allows understanding the process of the formation of wood accumulations in rivers. The experiments in this study focus on accumulations upstream of a vertical retention rack, common in intakes. Therefore, it is important to highlight that regular maintenance of reservoirs and retention structures is key to preventing accumulation, including preventing these pieces from absorbing water and increasing their weight.

Acknowledgements

Author contributions (CRediT)

Maggie R. Mallqui: Conceptualization, Methodology, Software, Validation, Formal Analysis, Investigation, Resources, Data Curation, Writing - Original Draft, Visualization. Erick Claros: Software, Formal analysis, Writing - Original Draft, Writing - Review & Editing, Visualization. Juan Cabrera: Conceptualization, Methodology, Writing - Review & Editing, Supervision

Data Access Statement

The data corresponding to the measurements and the characteristics of 3D printing is available at the following link: Online Repository.

Notations

Name	Symbol	Unit
Approach flow depth	h_o	m
Increase of flow depth	Δh	m
Approach flow Froude number	F_o	
Froude number with wood accumulation present	F_A	
Discharge	Q	m³/s
Velocity	v	m/s
Channel slope	s	
Log density	ρ_L	kg/m³
Water density	ρ_W	kg/m³
Log length	L_L	m
Log diameter	d_L	m
Solid volume	V_s	m³
Loose volume	V_l	m³
Characteristic volume	V_c	m³
Accumulation type factor	f_A	
Organic fine material fraction	FM	
Channel width	B	m
Accumulation thickness	T_A	m
Accumulation length	L_A	m
Compactness coefficient	$C_{T/L}$	
Coefficient of the adapted equation	C_1	
Exponents of the adapted equation	k_i	
Exponents of compactness equation	m, n	
Bulk factor	a	
Acceleration of gravity	g	m/s²
Accumulation compactness	T_A/L_A	
Relative standard error	$e*$	%
Flow diversion	μ	

References

Al-Zawaidah, H., Ravazzolo, D., & Friedrich, H. (2021). Local geomorphic effects in the presence of accumulations of different densities. *Geomorphology*, *389*, 14. https://doi.org/10.1016/j.geomorph.2021.107838

Braudrick, C. A., & Grant, G. E. (2000). When do logs move in rivers? *Water Resources Research*, *36*(2), 571–583. https://doi.org/10.1029/1999WR900290

Chow, V. Te. (1959). *Hidráulica de canales abiertos* (M. E. Suárez R., Ed.; Mc Graw Hi).

Consorcio Hidrovia Huallaga. (2005). Estudio de Navegabilidad del río Huallaga, en el tramo comprendido entre Yurimaguas y la confluencia con el río Marañón. Ministerio de Transportes y Telecomunicaciones. Lima, Perú.

Follett, E., Schalko, I., & Nepf, H. (2021). Logjams With a Lower Gap: Backwater Rise and Flow Distribution Beneath and Through Logjam Predicted by Two-Box Momentum Balance. *Geophysical Research Letters*, *48*(16), 1–10. https://doi.org/10.1029/2021GL094279

Furlan, P. (2019). Blocking probability of large wood and resulting head increase at ogee crest spillways (PhD. Thesis). Escuela Politécnica Federal de Lausana, Suiza.

Gschnitzer, T., Gems, B., Mazzorana, B., & Aufleger, M. (2017). Towards a robust assessment of bridge clogging processes in flood risk management. *Geomorphology*, *279*, 128–140. https://doi.org/10.1016/j.geomorph.2016.11.002

Gurnell, A. M., Piégay, H., Swanson, F. J., & Gregory, S. V. (2002). Large wood and fluvial processes. *Freshwater Biology*, *47*(4), 601–619. https://doi.org/10.1046/j.1365-2427.2002.00916.x

Hartlieb, A. (2017a). Decisive Parameters for Backwater Effects Caused by Floating Debris Jams. *Open Journal of Fluid Dynamics*, *07*(04), 475–484. https://doi.org/10.4236/ojfd.2017.74032

Hartlieb, A. (2017b). Decisive Parameters for Backwater Effects Caused by Floating Debris Jams. *Open Journal of Fluid Dynamics*, *07*(04), 475–484. https://doi.org/10.4236/ojfd.2017.74032

Hartlieb, Arnd. (2015). Schwemmholz in Fließgewässern : Gefahren und Lösungsmöglichkeiten. TUM.

Lange, D., & Bezzola, G. R. (2006). Schwemmholz: Probleme und Lösungsansätze ('Large wood: problems and approach methods'). In *VAW-Report 188 (Meyer-Peter, ed)*.

Livers, B., Lininger, K. B., Kramer, N., & Sendrowski, A. (2020). Porosity problems: Comparing and reviewing methods for estimating porosity and volume of wood jams in the field. *Earth Surface Processes and Landforms*, *45*(13), 3336–3353. https://doi.org/10.1002/esp.4969

Lucía, A., Comiti, F., Borga, M., Cavalli, M., & Marchi, L. (2015). Dynamics of large wood during a flash flood in two mountain catchments Dynamics of large wood during a flash flood in two mountain catchments. *Natural Hazards and Earth System Sciences*, *15*, 1741–1755. https://doi.org/10.5194/nhess-15-1741-2015

Moya Roque, R., Gómez Cortes, M., & Rivero Moreno, J. (2008). Clave de identificación macroscópica para 22 especies maderables de Bolivia. *Revista Forestal Venezolana*, *51*(2), 179–193.

Panici, D., & de Almeida, G. A. M. (2018). Formation, Growth, and Failure of Debris Jams at Bridge Piers. *Water Resources Research*, *54*(9), 6226–6241. https://doi.org/10.1029/2017WR022177

Ruiz-Villanueva, V., Piégay, H., Gaertner, V., Perret, F., & Stoffel, M. (2016). Wood density and moisture sorption and its influence on large wood mobility in rivers. *Catena*, *140*, 182–194. https://doi.org/10.1016/j.catena.2016.02.001

Schalko, I., Lageder, C., Schmocker, L., Weitbrecht, V., & Boes, R. M. (2019a). I Laboratory Flume Experiments on the Formation of Spanwise Large Wood Accumulations: I. Effect on Backwater Rise. *Water Resources Research*, *55*(6), 4854–4870. https://doi.org/10.1029/2018WR024649

Schalko, I., Lageder, C., Schmocker, L., Weitbrecht, V., & Boes, R. M. (2019b). I Laboratory Flume Experiments on the Formation of Spanwise Large Wood Accumulations: I. Effect on Backwater Rise. *Water Resources Research*, *55*(6), 4854–4870. https://doi.org/10.1029/2018WR024649

Schalko, I., Ruiz-Villanueva, V., & Maager, F. (2021). Wood Retention at Inclined Bar Screens: Effect of Wood Characteristics on Backwater Rise and Bedload Transport. *MDPI*, *13*, 1–16.

Schalko, I., Schmocker, L., Weitbrecht, V., & Boes, R. M. (2018a). Backwater rise due to large wood accumulations. *Journal of Hydraulic Engineering*, *144*(9), 1–13. https://doi.org/10.1061/(ASCE)HY.1943-7900.0001501

Schalko, I., Schmocker, L., Weitbrecht, V., & Boes, R. M. (2018b). Backwater rise due to large wood accumulations. *Journal of Hydraulic Engineering*, *144*(9), 1–13. https://doi.org/10.1061/(ASCE)HY.1943-7900.0001501

Schmocker, L., & Hager, W. H. (2013). Scale modeling of wooden debris accumulation at a debris rack. *Journal of Hydraulic Engineering*, *139*(8), 827–836. https://doi.org/10.1061/(ASCE)HY.1943-7900.0000714